



## Communication

# A Novel Thiosemicarbazide-Based Fluorescent Chemosensor for Hypochlorite in Near-Perfect Aqueous Solution and Zebrafish

Minji Lee <sup>1</sup>, Donghwan Choe <sup>1</sup> , Soyoung Park <sup>1</sup>, Hyeongjin Kim <sup>1</sup>, Soomin Jeong <sup>2</sup>, Ki-Tae Kim <sup>2,\*</sup>  and Cheal Kim <sup>1,\*</sup>

<sup>1</sup> Department of Fine Chemistry, Seoul National University of Science and Technology, Seoul 137-743, Korea; hye6455@seoultech.ac.kr (M.L.); 20510041@seoultech.ac.kr (D.C.); soyoung1119@seoultech.ac.kr (S.P.); adkd123@seoultech.ac.kr (H.K.)

<sup>2</sup> Department of Environmental Engineering, Seoul National University of Science and Technology, Seoul 01187, Korea; soomin\_jeong@seoultech.ac.kr

\* Correspondence: ktkim@seoultech.ac.kr (K.-T.K.); chealkim@snut.ac.kr (C.K.); Tel.: +82-2-960-6693 (K.-T.K.); +82-2-972-6640 (C.K.)

**Abstract:** A novel thiosemicarbazide-based fluorescent sensor (AFC) was developed. It was successfully applied to detect hypochlorite ( $\text{ClO}^-$ ) with fluorescence quenching in bis-tris buffer. The limit of detection of AFC for  $\text{ClO}^-$  was analyzed to be 58.7  $\mu\text{M}$ . Importantly, AFC could be employed as an efficient and practical fluorescent sensor for  $\text{ClO}^-$  in water sample and zebrafish. Moreover, AFC showed a marked selectivity to  $\text{ClO}^-$  over varied competitive analytes with reactive oxygen species. The detection process of AFC to  $\text{ClO}^-$  was illustrated by UV-visible and fluorescent spectroscopy and electrospray ionization-mass spectrometry (ESI-MS).

**Keywords:** thiosemicarbazide; hypochlorite; fluorescent chemosensor; acridine



**Citation:** Lee, M.; Choe, D.; Park, S.; Kim, H.; Jeong, S.; Kim, K.-T.; Kim, C.

A Novel Thiosemicarbazide-Based Fluorescent Chemosensor for Hypochlorite in Near-Perfect Aqueous Solution and Zebrafish.

*Chemosensors* **2021**, *9*, 65.

<https://doi.org/10.3390/chemosensors9040065>

Received: 29 January 2021

Accepted: 25 March 2021

Published: 28 March 2021

**Publisher's Note:** MDPI stays neutral with regard to jurisdictional claims in published maps and institutional affiliations.



**Copyright:** © 2021 by the authors. Licensee MDPI, Basel, Switzerland. This article is an open access article distributed under the terms and conditions of the Creative Commons Attribution (CC BY) license (<https://creativecommons.org/licenses/by/4.0/>).

## 1. Introduction

Concern for the recognition of reactive oxygen species (ROS) has increased because of the significant role of ROS in physiological and pathological processes [1–3].  $\text{ClO}^-$ , which is one of the significant ROS, is critically important in the human immune system, and has effective antibacterial and anti-inflammatory properties [4–7]. In addition, quantification of  $\text{ClO}^-$  is so important in the environmental system because it is significantly used in industrial fields, for example, as disinfectant and bleaching agent [8–10]. Abnormal amounts of  $\text{ClO}^-$  in organisms cause several diseases, such as inflammation and cardiovascular disease [11–15]. Hence, it is absolutely critical to develop selective and practical sensors for determining the amount of  $\text{ClO}^-$  in life systems [16–20].

Various analytical methods for the detection of  $\text{ClO}^-$ , such as colorimetric analysis, fluorescent detection, electrochemistry, and spectrophotometry, have been developed so far [21–23]. Fluorescence analysis, one of the analytical methods, has the merits of high sensitivity, specificity, fast response time, and manageability [24–27]. A number of fluorescent  $\text{ClO}^-$  sensors have been developed in the past decade, with several functional groups like hydrazide, thioether, thione, thioester, and C=N bond [28–33]. Nevertheless, many of them have some problems, such as poor water solubility, complicated synthesis methods, and nonbiological application. Therefore, it is necessary to develop fluorescent chemosensors with good water solubility and biological application.

Acridine and its derivatives are good fluorophores for chemosensors with high fluorescence quantum yield [34,35]. Moreover, amino acridine could readily form conjugated Schiff bases with aldehyde or ketone through the imine formation [36–38]. On the other hand, thiourea moiety is hydrophilic and well known to interact with reactive oxygen species like  $\text{ClO}^-$  [39–43]. Hence, we expected that a compound with thiourea moiety

linked to amino acridine may be a water-soluble chemosensor capable of detecting ROS like hypochlorite.

Here, we present a distinctly hypochlorite-specific fluorescent chemosensor, **AFC**, based on acridine moiety. Sensor **AFC** showed obvious fluorescent quenching and spectral variation with  $\text{ClO}^-$ . In particular, **AFC** could monitor  $\text{ClO}^-$  in zebrafish and environmental samples. With ESI-MS (electrospray ionization-mass spectrometry) analysis and  $^1\text{H}$  NMR titration, the sensing process of **AFC** for  $\text{ClO}^-$  was proposed.

## 2. Experiments

### 2.1. Materials and Equipment

All the reagents and solvents used for synthesis and spectroscopic measurements were purchased from Sigma-Aldrich. A Varian spectrometer (Mercury) was used to get  $^{13}\text{C}$  NMR (100 MHz) and  $^1\text{H}$  NMR (400 MHz) spectra. Elemental analysis for C, H, N, and S was carried out by using a Vario Macro/Micro-Cube elemental analyzer. PerkinElmer UV/Visible and fluorescence spectrometers were employed for UV-VIS and fluorescent measurements. A single-quadrupole ACQUITY QDa was employed to get ESI mass data.

### 2.2. Synthesis of FHC (2-Formyl-N-(Furan-2-Ylmethyl)Hydrazine-1-Carbothioamide)

An amount of 2 mmol of furfuryl isothiocyanate was dissolved in EtOH (7 mL). Then, 2 mmol of formic hydrazide was added to the solution. The mixture was shaken until a pale-yellow-colored powder precipitated. The pale-yellowish powder was filtered and scrubbed with methanol and ether [44]. Yield, 65%.  $^1\text{H}$  NMR in  $\text{DMSO}-d_6$ : 9.88 (s, 1H), 9.40 (s, 1H), 7.98 (s, 1H), 7.95 (s, 1H), 7.56 (s, 1H), 6.38 (t, 1H), 6.23 (d, 1H), and 4.66 (s, 2H).

### 2.3. Synthesis of AFC ((E)-2-((Acridin-9-Ylimino)Methyl)-N-(Furan-2-Ylmethyl)Hydrazine-1-Carbothioamide)

An amount of  $1 \times 10^{-3}$  mol of **FHC** was dissolved in EtOH (7 mL). Then,  $1 \times 10^{-3}$  mol of 9-aminoacridine (**AAD**) was dissolved in the solution. The mixture was stirred overnight, until the yellow powder precipitated. The yellow powder filtered was scrubbed with ether. Yield, 48%.  $^1\text{H}$  NMR in  $\text{DMSO}-d_6$ ,  $\delta$ : 8.45 (s, 1H), 8.40 (d, 2H), 7.80 (d, 2H), 7.65 (m, 3H), 7.32 (t, 2H), 6.45 (m, 2H), and 5.17 (s, 2H).  $^{13}\text{C}$  NMR in  $\text{DMSO}-d_6$ :  $\delta$  = 166.0, 148.3, 148.1, 143.4, 141.8, 130.2, 128.0, 130.2, 128.0, 123.4, 121.7, 112.80, 110.8, 109.4, and 40.4 ppm. ESI mass:  $m/z$  calcd for  $[\text{C}_{20}\text{H}_{17}\text{N}_5\text{OS} + \text{H}^+ + \text{DMSO}]^+$ : 454.14; found, 454.47. Elemental analysis: calcd (%) for  $\text{C}_{20}\text{H}_{19}\text{N}_5\text{O}_2\text{S}$  (**AFC** +  $\text{H}_2\text{O}$ ): C, 61.05; H, 4.87; N, 17.80; S, 8.15; found (%): C, 60.96; H, 4.35; N, 17.44; S, 7.99.

### 2.4. General Procedures

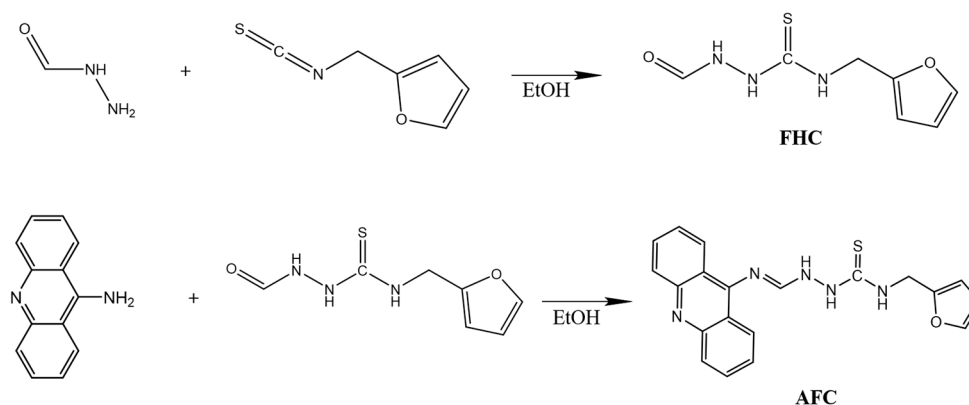
A stock solution of **AFC** was prepared by dissolving **AFC** (0.05 mmol) in DMSO (5.0 mL). An aqueous  $\text{NaClO}$  solution (500  $\mu\text{mol}$ , 11%) was diluted in distilled water to make a concentrated solution (100 mM). Stock solutions of varied anions and ROS were prepared in bis-tris buffer. Fluorescent and UV-visible data were recorded in a near-perfect aqueous media (10 mM, bis-tris, pH 7.0).

### 2.5. Imaging in Zebrafish

Under the previous conditions were cultured zebrafish embryos [45]. An amount of 66  $\mu\text{L}$  of a stock **AFC** solution (15.2 mM) was diluted to 20 mL bis-tris buffer. The zebrafish embryos (6 days old) were treated with the diluted **AFC** (50  $\mu\text{M}$ ) for 20 min and then smoothly washed with E2 media to get rid of the excess of **AFC**. Afterward, the zebrafish were divided into two groups. One was control group and the other group was experimental group. In the experimental group, the zebrafish were further dealt with 50  $\mu\text{M}$  of  $\text{ClO}^-$  for 15 min and scrubbed with E2 media. The zebrafish were narcotized by adding ethyl-3-aminobenzoate methanesulfonate. The fluorescence images of the zebrafish were obtained by a fluorescent microscope.

### 3. Results and Discussion

Chemosensor **AFC** was obtained by the imine formation reaction of 9-aminoacridine and **FHC** (Scheme 1). It was verified by  $^1\text{H}$  NMR,  $^{13}\text{C}$  NMR, and ESI-MS. The detecting process of **AFC** to  $\text{ClO}^-$  was studied by UV-VIS spectroscopy, fluorescent spectroscopy, and  $^1\text{H}$  NMR titration.



**Scheme 1.** Synthesis of **AFC**.

#### 3.1. Spectroscopic Investigations of Chemosensor **AFC** to $\text{ClO}^-$

We examined the fluorescent responses of **AFC** to varied anions ( $\text{Br}^-$ ,  $\text{CN}^-$ ,  $\text{S}^{2-}$ ,  $\text{I}^-$ ,  $\text{SCN}^-$ ,  $\text{OAc}^-$ ,  $\text{ClO}^-$ ,  $\text{F}^-$ ,  $\text{H}_2\text{PO}_4^-$ ,  $\text{N}_3^-$ ,  $\text{BzO}^-$ ,  $\text{NO}_2^-$ , and  $\text{Cl}^-$ ) and ROS species ( $\text{H}_2\text{O}_2$ ,  $\text{AcOOH}$ , and  $\text{tBuOOH}$ ) in buffer (Figure 1). Sensor **AFC** exhibited an intense fluorescence emission at 455 nm with excitation at 350 nm ( $\Phi = 0.8438$ ). When 290 equivalents of varied anions were added, respectively, to the **AFC** solution, only  $\text{ClO}^-$  induced a distinct decrease in fluorescence emission ( $\Phi = 0.0197$ ). By contrast, the other anions did not make substantial changes in fluorescent intensity, and  $\text{AcOOH}$  showed some increase in intensity at 455 nm. This result verified that chemosensor **AFC** could be served as an efficient fluorescent sensor for selectively detecting  $\text{ClO}^-$ .

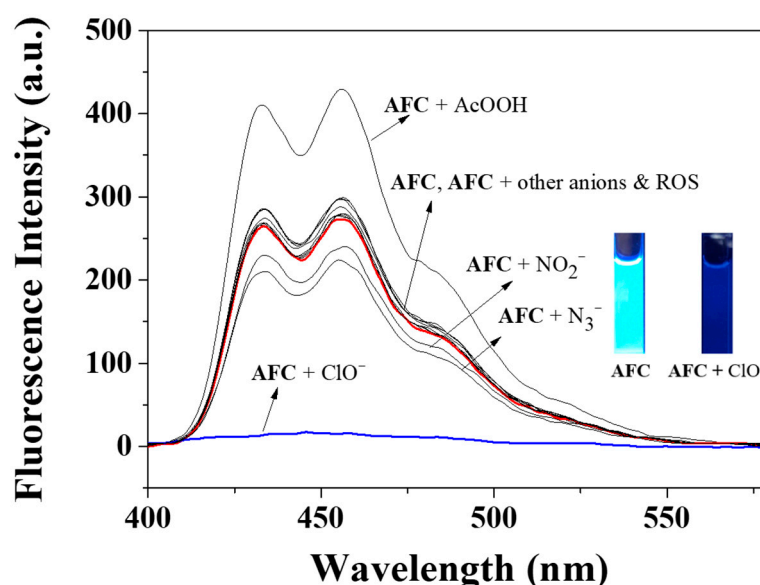


**Figure 1.** Fluorescent variations of **AFC** ( $1 \times 10^{-5}$  M) with various anions (290 equivalents).

Spectroscopic titrations were implemented to investigate the physical responses of **AFC** to  $\text{ClO}^-$  (Figure 2). In addition to  $\text{ClO}^-$ , the intensity of the fluorescence emission

of AFC at 455 nm gradually decreased, and the detection limit ( $C_{DL} = 3\sigma/k$ ) for  $\text{ClO}^-$  turned out to be  $58.7 \mu\text{M}$  (Figure S1). In the same way, UV–VIS titration was carried out (Figure 3). The result showed a consistent increase of absorbance at 320 and 490 nm and a decrease of absorbance at 400 nm with an apparent isosbestic point at 420 nm. In addition, the time-dependent UV–VIS change of AFC showed that AFC was stable enough for 1 h (Figure S2).

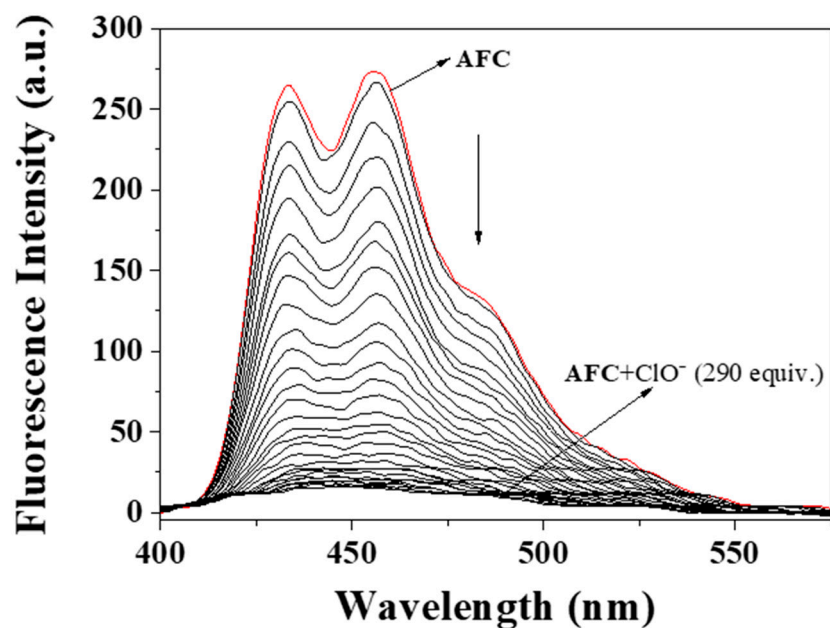


Figure 2. Fluorescent change of AFC ( $1 \times 10^{-5} \text{ M}$ ) with different amounts of  $\text{ClO}^-$  (from 0 to 290 equivalents).

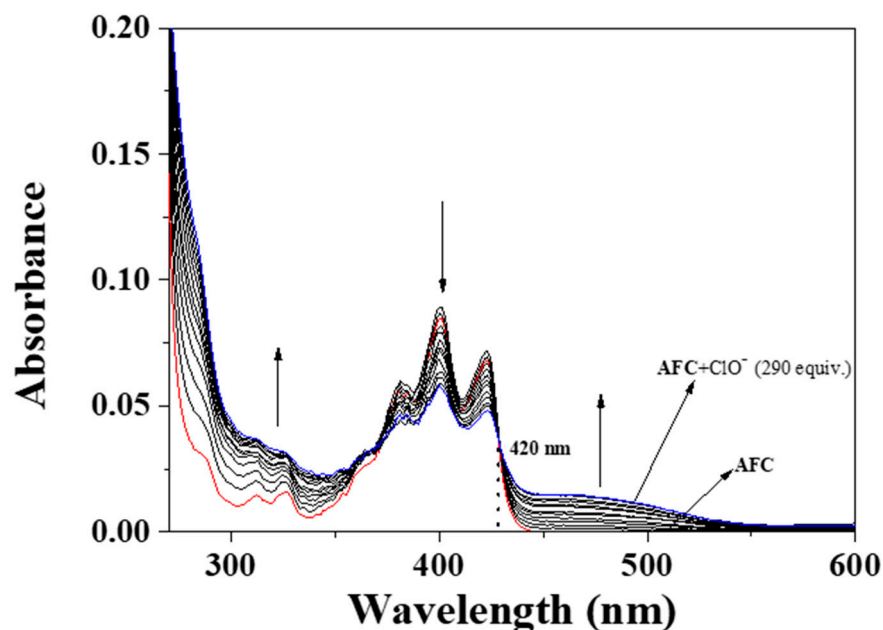


Figure 3. UV–VIS change of probe AFC ( $1 \times 10^{-5} \text{ M}$ ) with different amounts of  $\text{ClO}^-$ .

The binding process of AFC to  $\text{ClO}^-$  could be demonstrated with the result of the ESI-mass experiment (Figure S3). The peak at  $m/z = 211.294$  can be assigned as  $[\text{AAD-O} + \text{H}^+]^+$  (calcd,  $m/z = 211.090$ ). In addition, we can assign the peak at  $m/z = 232.287$  as

$[\text{FHC} + \text{MeOH} + \text{H}^+]^+$  (calcd,  $m/z = 232.080$ ). The outcome suggests that the C=N bond of **AFC** would be cleaved by  $\text{ClO}^-$  to produce **FHC** and **AAD**. Then, **AAD** was further oxidized to **AAD-O** by another  $\text{ClO}^-$ . To get more information on the cleavage of **AFC**,  $^1\text{H}$  NMR titration was conducted (Figure 4). Consequently, the imine proton ( $\text{H}_6$ ) of **AFC** disappeared due to the cleavage of the imine bond. The amine protons ( $\text{H}_5$  and  $\text{H}_{5'}$ ) of **AAD-O** and the aldehyde proton ( $\text{H}_{6'}$ ) of **FHC** appeared.

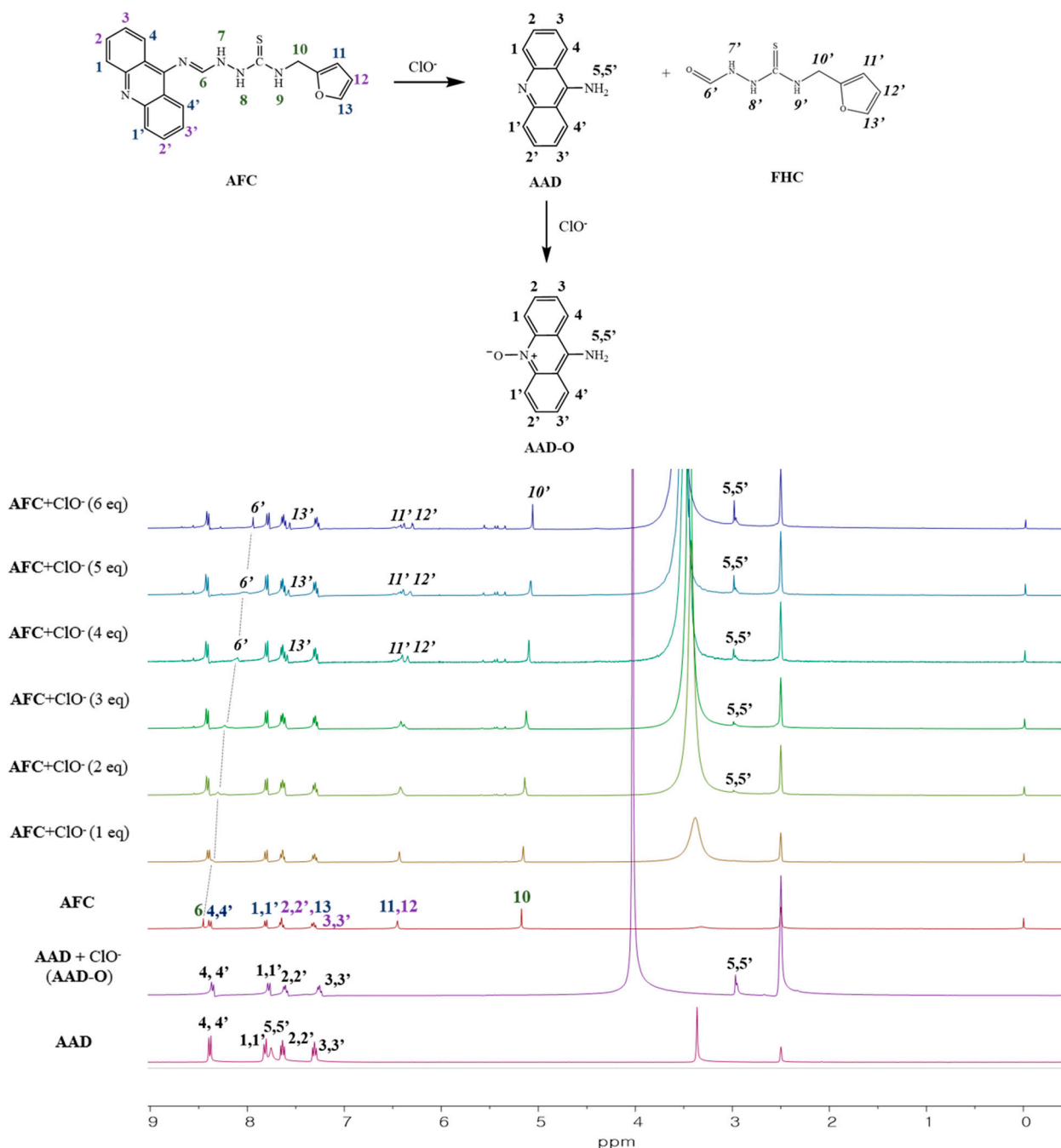
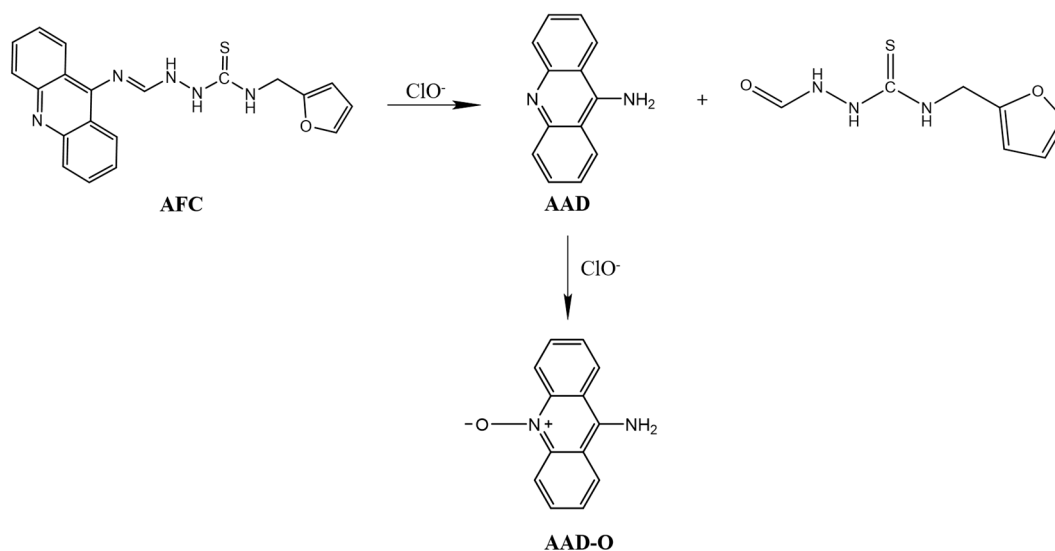


Figure 4.  $^1\text{H}$  NMR titration of **AFC** with  $\text{ClO}^-$  ( $\text{DMSO}-d_6$ ).

To further understand the sensing mechanism, we investigated the fluorescent and UV-VIS changes of **AAD** and **FHC** upon the addition of  $\text{ClO}^-$  (290 equivalents). The fluorescent intensity of **AAD** was substantially decreased by adding  $\text{ClO}^-$ , suggesting the oxidation of **AAD** into **AAD-O** (Figure S4). The UV-VIS spectra of **AAD** showed an

increase of absorbance at around 490 nm (Figure S5). On the other hand, **FHC** with/without  $\text{ClO}^-$  showed no fluorescence intensity and an increase in UV–VIS absorbance at 280 nm (Figures S6 and S7). Therefore, these observations and the results of the ESI–MS and  $^1\text{H}$  NMR titration drove us to propose that the  $\text{C}=\text{N}$  bond of **AFC** was cleaved by  $\text{ClO}^-$ , and then the resultant **AAD** was further oxidized to **AAD-O** by another  $\text{ClO}^-$  (Scheme 2).



**Scheme 2.** Sensing process of **AFC** by  $\text{ClO}^-$ .

To inspect the capability of **AFC** as a  $\text{ClO}^-$  sensor, we conducted a competitive test in the presence of  $\text{ClO}^-$  mixed with other anions of the same equivalents (Figure 5). The result demonstrated that all other analytes did not disturb the detection of  $\text{ClO}^-$  by **AFC**. Therefore, sensor **AFC** could be applied as an efficient chemosensor for  $\text{ClO}^-$  without the interference of other analytes. Moreover, the pH condition is critical for cellular behaviors and physiological processes. To evaluate the pH dependence of **AFC**, we measured fluorescent intensity in the range of pH 6–9 (Figure 6). **AFC** displayed intense fluorescence at pH 6–9, and the addition of  $\text{ClO}^-$  to **AFC** induced fluorescence quenching at pH 7–9. These outcomes imply that **AFC** could successfully detect  $\text{ClO}^-$  at pH 7–9. In addition, fluorescent analysis in the real samples including tap and drinking water was implemented for the practicality of probe **AFC**. The trustworthy values of recoveries and relative standard deviation (RSD) gave proof of the potential application of **AFC** to detect  $\text{ClO}^-$  in real samples (Table 1).

**Table 1.** Analysis of  $\text{ClO}^-$  <sup>a</sup>.

Sample	$\text{ClO}^-$ Added ( $\mu\text{M}$ )	$\text{ClO}^-$ Found ( $\mu\text{M}$ )	Recovery (%)	RSD ( $n = 3$ ) (%)
Drinking water	0.0	0.0		
	40.0 <sup>b</sup>	39.7	99.15	0.24
Tap water	0.0	0.00		
	40.0 <sup>c</sup>	38.3	95.64	0.18

<sup>a</sup> Condition:  $[\text{AFC}] = 1 \times 10^{-5}$  M in buffer (pH 7.0). <sup>b,c</sup> 40.0  $\mu\text{M}$  of  $\text{ClO}^-$  was artificially added.



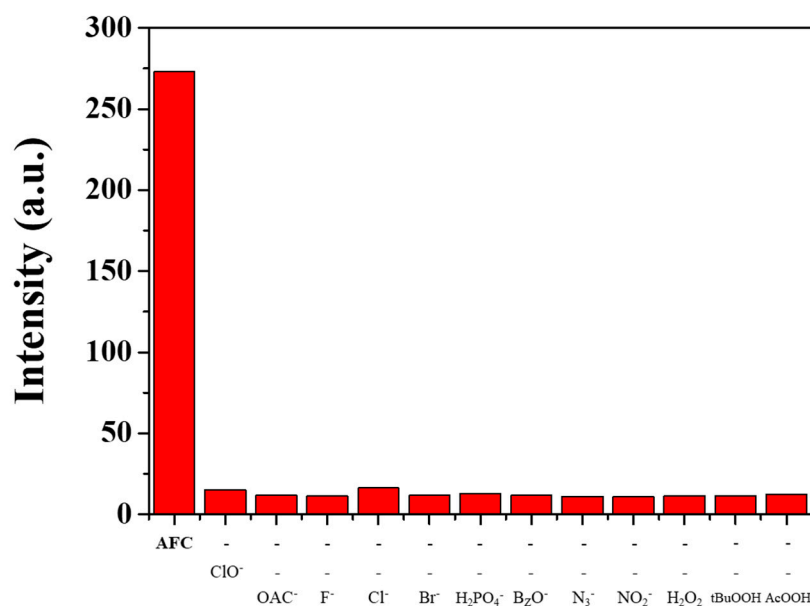


**Figure 5.** Competitive test (455 nm) of **AFC** ( $1 \times 10^{-5}$  M) to  $\text{ClO}^-$  (290 equivalents) in the presence of other anions (290 equivalents).

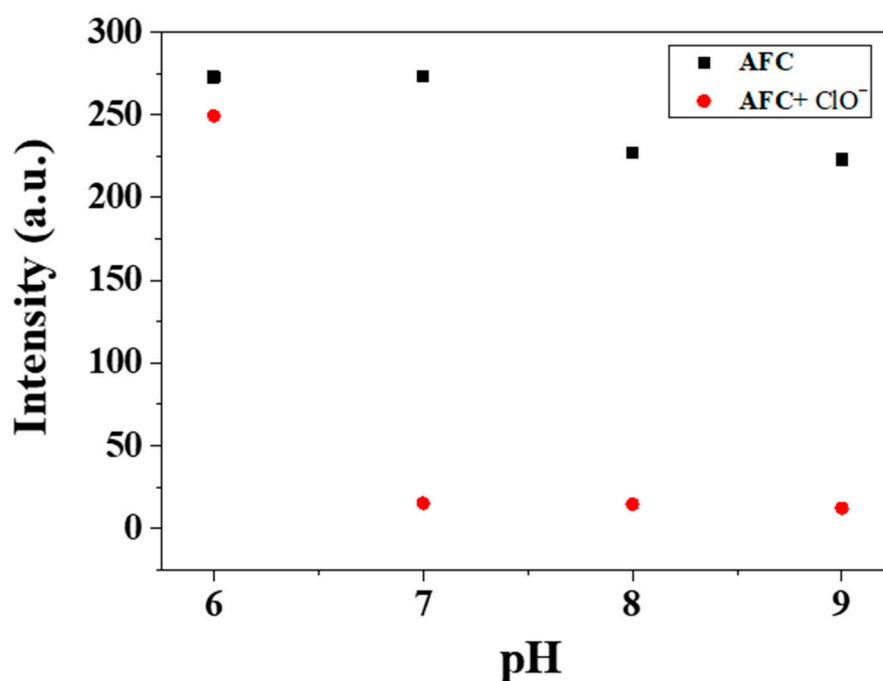


**Figure 6.** Fluorescence emission (at 455 nm) of **AFC** with  $\text{ClO}^-$  at pH 6–9.

### 3.2. In Vivo Imaging in Zebrafish

In order to test the sensing feasibility of the biological application of **AFC** to  $\text{ClO}^-$  fluorescent bioimaging, experiments were conducted with zebrafish (Figure 7). We first incubated zebrafish with **AFC** (50  $\mu\text{M}$ ), followed by treatment with  $\text{ClO}^-$  (50  $\mu\text{M}$ ). While the zebrafish treated with only probe **AFC** exhibited a green fluorescence in the swim bladder and eyes, the zebrafish with additional treatment of  $\text{ClO}^-$  showed no fluorescence signal. The bioimaging experiments demonstrated the detecting ability of **AFC** to trace  $\text{ClO}^-$  in living organisms. Importantly, **AFC** is the second fluorescent turnoff sensor for  $\text{ClO}^-$  applicable to both real water samples and zebrafish [46–51].

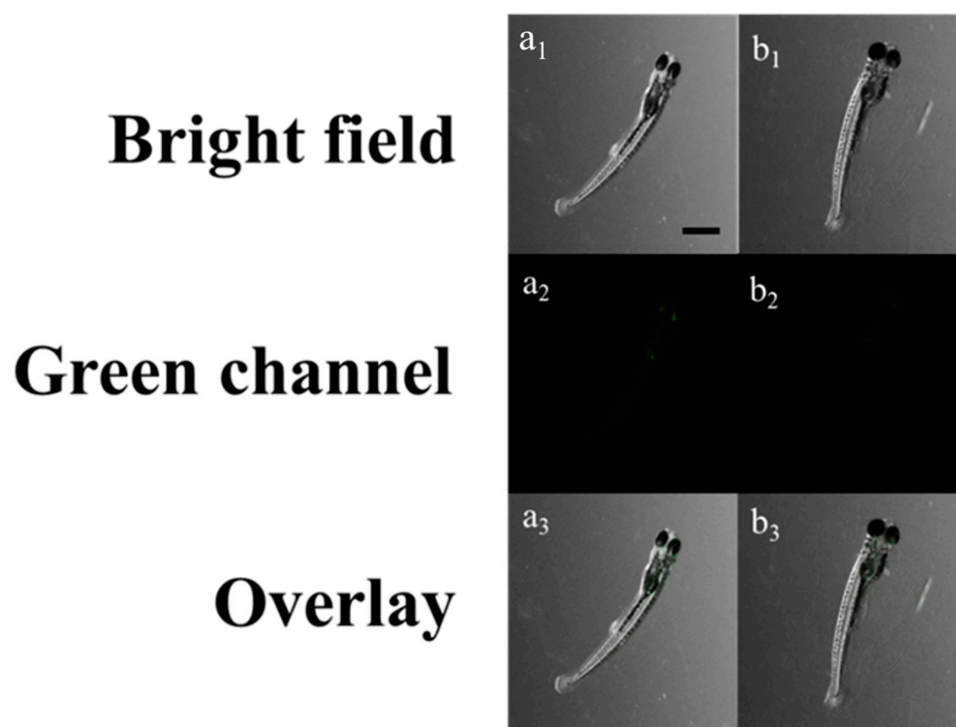


**Figure 7.** Fluorescence images of zebrafish (6 days old) treated with **AFC** followed by the addition of  $\text{ClO}^-$ . (**a**<sub>1</sub>–**a**<sub>3</sub>): **AFC** only; (**b**<sub>1</sub>–**b**<sub>3</sub>): **AFC** with  $5 \times 10^{-5}$  M  $\text{ClO}^-$ . [**AFC**] =  $5 \times 10^{-5}$  M.

#### 4. Conclusions

A novel thiosemicarbazide-based chemosensor **AFC** for detecting  $\text{ClO}^-$  was synthesized from the reaction of aminoacridine and a new aldehyde group synthesized from formic hydrazide. Probe **AFC** selectively recognized  $\text{ClO}^-$  over other anions including ROS in aqueous solution. With  $\text{ClO}^-$ , probe **AFC** showed remarkable fluorescence quenching. The limit of detection of **AFC** for  $\text{ClO}^-$  was calculated to be 58.7  $\mu\text{M}$ . Additionally, probe **AFC** could be applicable for quantitative analysis in real water samples and zebrafish. Importantly, **AFC** is the second fluorescent turnoff sensor for  $\text{ClO}^-$  applicable to both real water samples and zebrafish. The dependable results in this study shows that **AFC** could be used as an efficient chemosensor for detecting  $\text{ClO}^-$  in aqueous solution and small organisms by a fluorescent quenching method.

**Supplementary Materials:** The following are available online at <https://www.mdpi.com/article/10.3390/chemosensors9040065/s1>. Table S1: Fluorescent turnoff chemosensors for recognizing hypochlorite in aqueous solutions. Figure S1: Determination of the detection limit of **AFC** for  $\text{ClO}^-$  based on the change of intensity at 455 nm. Figure S2: The time-dependent UV–VIS change (400 nm) of **AFC** with/without  $\text{ClO}^-$ . Figure S3: Positive-ion ESI mass spectrum of **AFC** upon the addition of NaClO. **Figure S4:** Fluorescent change of **AAD** with/without  $\text{ClO}^-$ . Figure S5: UV–VIS change of **AAD** with/without  $\text{ClO}^-$ . Figure S6: Fluorescent change of **FHC** with/without  $\text{ClO}^-$ . Figure S7: UV–VIS change of **FHC** with/without  $\text{ClO}^-$ .

**Author Contributions:** Conceptualization, M.L. and C.K.; formal analysis, M.L.; investigation, M.L., D.C., H.K. and S.J.; data curation, M.L., S.P. and D.C.; writing—original draft preparation, M.L., D.C. and S.P.; writing—review and editing, M.L. and C.K.; supervision, C.K. and K.-T.K.; funding acquisition, C.K. and K.-T.K. All authors have read and agreed to the published version of the manuscript.

**Funding:** We acknowledge the Korea Environmental Industry and Technology Institute (KEITI) through “The Chemical Accident Prevention Technology Development Project”, funded by the Korean Ministry of Environment (MOE) (No. 2016001970001).



**Institutional Review Board Statement:** The maintenance of zebrafish was approved by the Institutional Animal Care and Use Committees at the Seoul National University of Science and Technology. Ethical review and approval were waived for this study because early-life stages of zebrafish (<120 hpf) are not protected according to the European Union (EU) Directive 2010/63/EU.

**Informed Consent Statement:** Not applicable.

**Conflicts of Interest:** The authors declare no conflict of interest.

## References

- Ji, R.; Qin, K.; Liu, A.; Zhu, Y.; Ge, Y. A simple and fast-response fluorescent probe for hypochlorite in living cells. *Tetrahedron Lett.* **2018**, *59*, 2372–2375. [\[CrossRef\]](#)
- Jiang, Y.; Zheng, G.; Duan, Q.; Yang, L.; Zhang, J.; Zhang, H.; He, J.; Sun, H.; Ho, D. Ultra-sensitive fluorescent probes for hypochlorite acid detection and exogenous/endogenous imaging of living cells. *Chem. Commun.* **2018**, *54*, 7967–7970. [\[CrossRef\]](#) [\[PubMed\]](#)
- Yun, D.; Chae, J.B.; Kim, C. An imine-based colorimetric chemodosimeter for the detection of hypochlorite ( $\text{ClO}^-$ ) in aqueous media: Its application in test strips and real water samples. *J. Chem. Sci.* **2019**, *131*, 1–8. [\[CrossRef\]](#)
- Lou, X.; Zhang, Y.; Qin, J.; Li, Z. Colorimetric hypochlorite detection using an azobenzene acid in pure aqueous solutions and real application in tap water. *Sens. Actuators B Chem.* **2012**, *161*, 229–234. [\[CrossRef\]](#)
- Shen, S.L.; Zhang, X.F.; Ge, Y.Q.; Zhu, Y.; Cao, X.Q. A mitochondria-targeting ratiometric fluorescent probe for the detection of hypochlorite based on the FRET strategy. *RSC Adv.* **2017**, *7*, 55296–55300. [\[CrossRef\]](#)
- Xu, X.; Qian, Y. A novel (3,6-di-tert-butylcarbazol-9-yl) triphenylamine-BODIPY-tricyanofuran conjugated dye: Synthesis and rapid naked-eye detection of hypochlorite. *New J. Chem.* **2017**, *41*, 9607–9612. [\[CrossRef\]](#)
- Yi, S.; Lu, Z.; Lin, Y.; Wang, J.; Qiao, Z.; Shen, R.; Zhang, J.; Hou, L. A novel mitochondria-targeted phosphorescence probe for hypochlorite ions detection in living cells. *Talanta* **2020**, *209*, 120516. [\[CrossRef\]](#) [\[PubMed\]](#)
- Lee, S.C.; Kim, C. Naphthalimide-based probe for the detection of hypochlorite in a near-perfect aqueous solution. *Anal. Sci.* **2019**, *35*, 1189–1193. [\[CrossRef\]](#)
- Goswami, S.; Paul, S.; Manna, A. Carbazole based hemicyanine dye for both “naked eye” and ‘NIR’ fluorescence detection of  $\text{CN}^-$  in aqueous solution: From molecules to low cost devices (TLC plate sticks). *Dalton Trans.* **2013**, *42*, 10682–10686. [\[CrossRef\]](#)
- Lee, S.C.; Kim, C. Naphthol-naphthalimide based ‘turn-on’ fluorescent sensor for  $\text{ClO}^-$  in aqueous media and test kit. *Inorg. Chem. Commun.* **2019**, *108*, 107545. [\[CrossRef\]](#)
- Sasikumar, T.; Ilanchelian, M. Colorimetric detection of hypochlorite based on the morphological changes of silver nanoprisms to spherical nanoparticles. *Anal. Methods* **2017**, *9*, 3151–3158. [\[CrossRef\]](#)
- Chen, W.C.; Venkatesan, P.; Wu, S.P. A highly selective turn-on fluorescent probe for hypochlorous acid based on hypochlorous acid-induced oxidative intramolecular cyclization of boron dipyrromethene-hydrazone. *Anal. Chim. Acta* **2015**, *882*, 68–75. [\[CrossRef\]](#)
- Duan, R.; Li, C.; Liu, S.; Liu, Z.; Li, Y.; Zhu, J.; Hu, X. A selective fluorescence quenching method for the determination of trace hypochlorite in water samples with Nile blue A. *J. Taiwan Inst. Chem. Eng.* **2015**, *50*, 43–48. [\[CrossRef\]](#)
- Lin, X.; Qin, W.; Chen, Y.; Bao, L.; Li, N.; Wang, S.; Liu, K.; Kong, F.; Yi, T. Construction of a multi-signal near-infrared fluorescent probe for sensing of hypochlorite concentration fluctuation in living animals. *Sens. Actuators B Chem.* **2020**, *324*. [\[CrossRef\]](#)
- Zhang, Y.M.; Fang, H.; Zhu, W.; He, J.X.; Yao, H.; Wei, T.B.; Lin, Q.; Qu, W.J. Ratiometric fluorescent sensor based oxazolo-phenazine derivatives for detect hypochlorite via oxidation reaction and its application in environmental samples. *Dyes Pigm.* **2020**, *172*, 107765. [\[CrossRef\]](#)
- Chang, C.; Wang, F.; Qiang, J.; Zhang, Z.; Chen, Y.; Zhang, W.; Wang, Y.; Chen, X. Benzothiazole-based fluorescent sensor for hypochlorite detection and its application for biological imaging. *Sens. Actuators B Chem.* **2017**, *243*, 22–28. [\[CrossRef\]](#)
- Starzak, K.; Matwijczuk, A.; Creaven, B.; Matwijczuk, A.; Wybraniec, S.; Karcz, D. Fluorescence quenching-based mechanism for determination of hypochlorite by coumarin-derived sensors. *Int. J. Mol. Sci.* **2019**, *20*, 281. [\[CrossRef\]](#) [\[PubMed\]](#)
- Wang, W.; Ning, J.Y.; Liu, J.T.; Miao, J.Y.; Zhao, B.X. A mitochondria-targeted ratiometric fluorescence sensor for the detection of hypochlorite in living cells. *Dyes Pigm.* **2019**, *171*, 107708. [\[CrossRef\]](#)
- Naha, S.; Varalakshmi, A.; Velmathi, S. Nanomolar colorimetric hypochlorite sensor in water. *Spectrochim. Acta Part A Mol. Biomol. Spectrosc.* **2019**, *220*, 117123. [\[CrossRef\]](#)
- Hwang, S.M.; Yun, D.; Kim, C. An Imidazo[1,5- $\alpha$ ]Pyridine-Based Fluorometric Chemodosimeter for the Highly Selective Detection of Hypochlorite in Aqueous Media. *J. Fluoresc.* **2019**, *29*, 451–459. [\[CrossRef\]](#)
- Zhang, P.; Wang, H.; Hong, Y.; Yu, M.; Zeng, R.; Long, Y.; Chen, J. Selective visualization of endogenous hypochlorous acid in zebrafish during lipopolysaccharide-induced acute liver injury using a polymer micelles-based ratiometric fluorescent probe. *Biosens. Bioelectron.* **2018**, *99*, 318–324. [\[CrossRef\]](#) [\[PubMed\]](#)
- Li, J.; Yin, C.; Liu, T.; Wen, Y.; Huo, F. A new mechanism-based fluorescent probe for the detection of  $\text{ClO}^-$  by UV-vis and fluorescent spectra and its applications. *Sens. Actuators B Chem.* **2017**, *252*, 1112–1117. [\[CrossRef\]](#)

23. Dong, X.; Zhang, G.; Shi, J.; Wang, Y.; Wang, M.; Peng, Q.; Zhang, D. A highly selective fluorescence turn-on detection of  $\text{ClO}^-$  with 1-methyl-1,2-dihydropyridine-2-thione unit modified tetraphenylethylene. *Chem. Commun.* **2017**, *53*, 11654–11657. [[CrossRef](#)] [[PubMed](#)]
24. Hwang, S.M.; Kim, A.; Kim, C. A simple hydrazine-based probe bearing anthracene moiety for the highly selective detection of hypochlorite. *Inorg. Chem. Commun.* **2019**, *101*, 1–5. [[CrossRef](#)]
25. Jeong, H.Y.; Lee, S.Y.; Kim, C. Furan and Julolidine-Based “Turn-on” Fluorescence Chemosensor for Detection of  $\text{F}^-$  in a Near-Perfect Aqueous Solution. *J. Fluoresc.* **2017**, *27*, 1457–1466. [[CrossRef](#)]
26. Yang, Q.; Zhong, X.; Chen, Y.; Yang, J.; Jin, C.; Jiang, Y. A mitochondria-targeted fluorescent probe for hypochlorite sensing and its application in bioimaging. *Analyst* **2020**, *145*, 3100–3105. [[CrossRef](#)]
27. Feng, A.; Liu, P.; Liang, Q.; Zhang, X.; Huang, L.; Jia, Y.; Xie, M.; Yan, Q.; Li, C.; Wang, S. A new carbazole-based colorimetric and ratiometric fluorescent probe for hypochlorite sensing in living cells and zebrafishes. *Dyes Pigm.* **2020**, *180*, 108492. [[CrossRef](#)]
28. Ma, Z.; Chen, X.; Wang, C.; Lv, Q. A novel ratiometric fluorescence probe for hypochlorite detection and its application in cell imaging. *J. Mol. Struct.* **2020**, *1221*, 128812. [[CrossRef](#)]
29. Ning, Y.; Cui, J.; Lu, Y.; Wang, X.; Xiao, C.; Wu, S.; Li, J.; Zhang, Y. De novo design and synthesis of a novel colorimetric fluorescent probe based on naphthalenone scaffold for selective detection of hypochlorite and its application in living cells. *Sens. Actuators B Chem.* **2018**, *269*, 322–330. [[CrossRef](#)]
30. Zhou, J.; Li, L.; Shi, W.; Gao, X.; Li, X.; Ma, H. HOCl can appear in the mitochondria of macrophages during bacterial infection as revealed by a sensitive mitochondrial-targeting fluorescent probe. *Chem. Sci.* **2015**, *6*, 4884–4888. [[CrossRef](#)]
31. Dai, Y.; Xu, K.; Li, Q.; Wang, C.; Liu, X.; Wang, P. Acridine-based complex as amino acid anion fluorescent sensor in aqueous solution. *Spectrochim. Acta Part A Mol. Biomol. Spectrosc.* **2016**, *157*, 1–5. [[CrossRef](#)] [[PubMed](#)]
32. Jin, X.; Jia, Y.; Chen, W.; Chui, P.; Yang, Z. A reaction-based fluorescent probe for rapid detection of hypochlorite in tap water, serum, and living cells. *Sens. Actuators B Chem.* **2016**, *232*, 300–305. [[CrossRef](#)]
33. Wang, B.; Chen, D.; Kambam, S.; Wang, F.; Wang, Y.; Zhang, W.; Yin, J.; Chen, H.; Chen, X. A highly specific fluorescent probe for hypochlorite based on fluorescein derivative and its endogenous imaging in living cells. *Dyes Pigm.* **2015**, *120*, 22–29. [[CrossRef](#)]
34. Wang, C.; Wang, P.; Liu, X.; Fu, J.; Xue, K.; Xu, K. Novel enantioselective fluorescent sensors for tartrate anion based on acridinezswsxa. *Luminescence* **2017**, *32*, 1313–1318. [[CrossRef](#)] [[PubMed](#)]
35. Chemate, S.; Erande, Y.; Mohbiya, D.; Sekar, N. Acridine derivative as a “turn on” probe for selective detection of picric acid: Via PET deterrence. *RSC Adv.* **2016**, *6*, 84319–84325. [[CrossRef](#)]
36. Kim, M.S.; Lee, S.Y.; Jung, J.M.; Kim, C. A new Schiff-base chemosensor for selective detection of  $\text{Cu}^{2+}$  and  $\text{Co}^{2+}$  and its copper complex for colorimetric sensing of  $\text{S}^{2-}$  in aqueous solution. *Photochem. Photobiol. Sci.* **2017**, *16*, 1677–1689. [[CrossRef](#)] [[PubMed](#)]
37. Bhattacharyya, A.; Ghosh, S.; Makhal, S.C.; Guchhait, N. Hydrazine bridged coumarin-pyrimidine conjugate as a highly selective and sensitive  $\text{Zn}^{2+}$  sensor: Spectroscopic unraveling of sensing mechanism with practical application. *Spectrochim. Acta Part A Mol. Biomol. Spectrosc.* **2017**, *183*, 306–311. [[CrossRef](#)]
38. Ashraf, A.; Khizar, M.; Islam, M.; Hameed, A.; Tarique Moin, S.; Yaqub, M.; Rauf, W.; Moazzam Naseer, M.; Tayyeb Ahsan, M.; Shafiq, Z.; et al. Synthesis of sensitive novel dual Signaling pyridopyrimidine-based fluorescent “turn off” chemosensors for anions determination. *Meas. J. Int. Meas. Confed.* **2019**, *151*, 107267. [[CrossRef](#)]
39. Swamy, K.M.K.; Eom, S.; Liu, Y.; Kim, G.; Lee, D.; Yoon, J. Rhodamine derivatives bearing thiourea groups serve as fluorescent probes for selective detection of ATP in mitochondria and lysosomes. *Sens. Actuators B Chem.* **2019**, *281*, 350–358. [[CrossRef](#)]
40. So, H.; Lee, M.; Kim, C. A Unique Thiosemicarbazide-Based Colorimetric Chemosensor for  $\text{Fe}^{2+}$  in Pure Aqueous Solution with the Lowest Detection Limit. *ChemistrySelect* **2020**, *5*, 10521–10525. [[CrossRef](#)]
41. Shen, B.X.; Qian, Y.; Qi, Z.Q.; Lu, C.G.; Sun, Q.; Xia, X.; Cui, Y.P. Near-infrared BODIPY-based two-photon  $\text{ClO}^-$  probe based on thiosemicarbazide desulfurization reaction: Naked-eye detection and mitochondrial imaging. *J. Mater. Chem. B* **2017**, *5*, 5854–5861. [[CrossRef](#)]
42. Zeng, Y.N.; Zheng, H.Q.; He, X.H.; Cao, G.J.; Wang, B.; Wu, K.; Lin, Z.J. Dual-emissive metal-organic framework: A novel turn-on and ratiometric fluorescent sensor for highly efficient and specific detection of hypochlorite. *Dalton Trans.* **2020**, *49*, 9680–9687. [[CrossRef](#)] [[PubMed](#)]
43. Li, C.; Yin, P.; Li, T.; Wei, T.; Hu, T.; Chen, J.; Qin, X.; Niu, Q. Rapid and sensitive detection of hypochlorite in ~100% aqueous solution using a bithiophene-based fluorescent sensor: Application to water analysis and live-cell imaging. *J. Mol. Liq.* **2020**, *320*, 114396. [[CrossRef](#)]
44. Cai, W.; Wu, J.; Liu, W.; Xie, Y.; Liu, Y.; Zhang, S.; Xu, W.; Tang, L.; Wang, J.; Zhao, G. Systematic structure-activity relationship (SAR) exploration of diarylmethane backbone and discovery of a highly potent novel uric acid transporter 1 (URAT1) inhibitor. *Molecules* **2018**, *23*, 252. [[CrossRef](#)] [[PubMed](#)]
45. Kim, M.S.; Yun, D.; Chae, J.B.; So, H.; Lee, H.; Kim, K.; Kim, M.; Lim, M.H.; Kim, C. A Novel Thiophene-Based Fluorescent Chemosensor for the Detection of  $\text{Zn}^{2+}$  and  $\text{CN}^-$ : Imaging Applications in Live Cells and Zebrafish. *Sensors* **2019**, *19*, 5458. [[CrossRef](#)] [[PubMed](#)]
46. Chen, H.; He, X.; Yu, Y.; Qian, Y.; Shen, J.; Zhao, S. Execution of aggregation-induced emission as nano-sensors for hypochlorite detection and application for bioimaging in living cells and zebrafish. *Talanta* **2020**, *214*, 120842. [[CrossRef](#)]
47. So, H.; Lee, H.; Lee, G.D.; Kim, M.; Lim, M.H.; Kim, K.T.; Kim, C. A thiourea-based fluorescent chemosensor for bioimaging hypochlorite. *J. Ind. Eng. Chem.* **2020**, *89*, 436–441. [[CrossRef](#)]

- 
48. Zhu, Y.; Ma, Y.; Liu, Y.; Liu, Z.; Ma, S.; Xing, M.; Cao, D.; Lin, W. Fluorescence response of a fluorescein derivative for hypochlorite ion and its application for biological imaging in wounded zebrafish and living mice. *Sens. Actuators B Chem.* **2021**, *327*, 128848. [[CrossRef](#)]
  49. Zhang, Y.; Zuo, Y.; Yang, T.; Gou, Z.; Wang, X.; Lin, W. Novel fluorescent probe with a bridged Si-O-Si bond for the reversible detection of hypochlorous acid and biothiol amino acids in live cells and zebrafish. *Analyst* **2019**, *144*, 5075–5080. [[CrossRef](#)] [[PubMed](#)]
  50. Niu, H.; Chen, K.; Xu, J.; Zhu, X.; Cao, W.; Wang, Z.; Ye, Y.; Zhao, Y. Mitochondria-targeted fluorescent probes for oxidative stress imaging. *Sens. Actuators B Chem.* **2019**, *299*, 126938. [[CrossRef](#)]
  51. Lee, S.C.; Park, S.; So, H.; Lee, G.; Kim, K.T.; Kim, C. An acridine-based fluorescent sensor for monitoring  $\text{ClO}^-$  in water samples and zebrafish. *Sensors* **2020**, *20*, 4764. [[CrossRef](#)] [[PubMed](#)]